

Alternative method for wave propagation analysis within bounded linear media: conceptual and practical implications

Alberto Lencina,^{1,*} Beatriz Ruiz,² and Pablo Vaveliuk³

¹*Departamento de Física, Centro de Ciências Exatas e da Natureza, Universidade Federal da Paraíba, Caixa Postal 5008 CEP 58051-970, João Pessoa, Brazil.*

²*Centro de Investigaciones Ópticas, cc 124 (1900), La Plata, Argentina.*

³*Departamento de Física, Universidade Estadual de Feira de Santana, Campus Universitário BR 166 KM 03, 44031-460 Feira de Santana, Bahia, Brazil.*

(Dated: February 9, 2020)

This paper uses an alternative approach to study the monochromatic plane wave propagation within dielectric and conductor linear media of plane-parallel-faces. This approach introduces the time-averaged Poynting vector modulus as field variable. The conceptual implications of this formalism are that the nonequivalence between the time-averaged Poynting vector and the squared-field amplitude modulus is naturally manifested as a consequence of interface effects. Also, two practical implications are considered: first, the exact transmittance is compared with that given by the Beer's Law, employed commonly in experiments. The departure among them can be significative for certain material parameter values. Second, when the exact reflectance is studied for negative permittivity slabs, it is show that the high reflectance can be diminished if a small amount of absorption is present.

PACS numbers: 41.20.Jb, 42.25.Bs, 41.85.Ew

I. INTRODUCTION

The counter-propagating wave approach is commonly used to study the electromagnetic response of spatially nondispersive, homogeneous and isotropic plane-parallel-faces linear media (Fabry-Perot framework). It consider forward and backward monochromatic plane waves to derive the optical properties as the transmittance and reflectance [1]. This method uses the conventional variables of electromagnetic fields: moduli and phases of these waves which should be found from the Helmholtz equation with the corresponding boundary conditions. It is well-known that for a single harmonic plane wave propagating through an unbounded linear medium, the time-averaged Poynting vector modulus is equivalent to the squared-field amplitude modulus [2]. This statement is generally accepted even if the wave propagation takes place in bounded linear media. The counter-propagating approach does not point out the possible nonequivalence between the above magnitudes since utilizes the amplitudes and phases as field variables. However, the phase of the wave can be replaced by the time-averaged Poynting vector modulus as field variable. Then the time-averaged Poynting vector and the squared-field amplitude modulus can be monitored simultaneously within the medium so that the conditions that leads to the nonequivalence among them will manifest naturally in this equivalent frame.

The so-called S-formalism use the time-averaged Poynting vector as a field variable. It was recently introduced [3] and applied to study the optical response of nonlin-

ear slabs. The nonequivalence between the time-averaged Poynting vector and the squared-field amplitude modulus was the key to define a nonlinear medium whose nonlinearity is proportional to the time-averaged Poynting vector modulus. Its transmittance was calculated and found to differ with that obtained for the Kerr medium, whose nonlinearity is proportional to the squared-field amplitude modulus. However, the method was not yet used to analyze the linear case. Therefore, the aim of this paper is to apply the S-Formalism to study the optical properties of homogeneous, isotropic and spatially non-dispersive dielectric as well as Ohmic conductor media, inside the Fabry-Perot frame complementing to the well-known results of this problem within the counter-propagating wave approach. The S-formalism shows, in direct form, how this non-equivalence is related to the superposition dynamic of opposite traveling waves which is only possible in bounded media. Also, the exact transmittance is compared with that given by the approximated Beer's Law, commonly used in experiments, and appreciable differences were found for certain material parameters values. Moreover, the reflectance of positive and negative permittivity media are considered and interesting results appears for small absorption when negative permittivity accounts.

It must be stressed that the S-formalism does not substitute the counter-propagating wave approach because the idea of forward and backward waves within the medium has a deep physical content. However, the alternative method adds conceptual and practical implications that remains hidden when the conventional scheme is utilized. We believe that both methods should be complementary, helping for a complete physical understanding on wave propagation in bounded linear media.

Below, this paper reviews the principal features of the

*Corresponding author. Electronic address: agl@fisica.ufpb.br

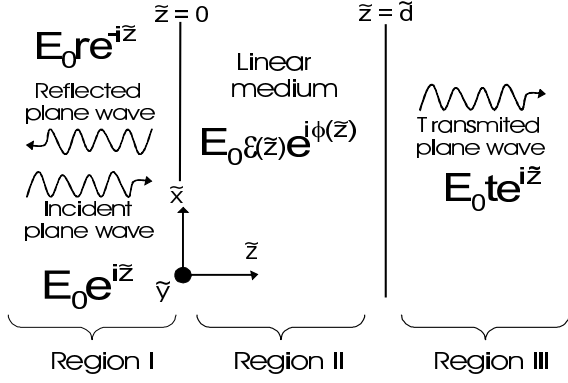


FIG. 1: A harmonic plane wave of amplitude E_0 , wave vector k_0 and frequency ω strikes a linear, non-magnetic, homogeneous, isotropic, and spatially non-dispersive plane-parallel-faces, to be reflected and transmitted. The field in Region II can be represented by a general complex field of real amplitude \mathcal{E} and phase ϕ . The Regions I and III constitute, for simplicity, the same linear dielectric medium (e.g., air). r and t are the reflection and transmission complex coefficients, respectively; $\tilde{z} = k_0 z$ is the dimensionless propagation coordinate.

S-Formalism introduced in Ref. 3 as function of the new set of field variables. Then, it is applied to derive the spatial evolution of both variables for absorbent and non-absorbent linear media showing the cases in which the equivalence does not hold true, and their causes and consequences. Finally, practical implications of this features are explored: the comparison between the exact transmittance and the Beer's law, and the analysis of positive and negative permittivity media.

II. S-FORMALISM APPROACH

When a linear, non-magnetic, homogeneous, isotropic, and spatially non-dispersive plane-parallel-faces medium of dimensionless thickness d ($= k_0 d$) is excited perpendicularly by a plane wave (see Fig. 1), the S-Formalism [3] states that the transmittance and reflectance are respectively

$$R = |r|^2 = 1 - S(0), \quad (1a)$$

$$T = |t|^2 = S(\tilde{d}), \quad (1b)$$

where S is the field variable, representing the dimensionless time-averaged Poynting vector modulus, given by

$$S(\tilde{z}) = \frac{\langle \mathbf{S} \rangle \cdot \hat{\mathbf{e}}_z}{I_0} = \mathcal{E}^2 \frac{d\phi}{d\tilde{z}} \quad (2)$$

where $I_0 = \epsilon_0 \omega / (2k_0) E_0^2$ is the incident intensity with ϵ_0 , the vacuum permittivity, $\hat{\mathbf{e}}_z$ the unit vector in the z direction, and \mathcal{E} and ϕ are the electric field amplitude modulus and phase, respectively. $S(\tilde{z})$ and $\mathcal{E}(\tilde{z})$ evolve

according to the coupled system [3]

$$\mathcal{E}^3 \frac{d^2 \mathcal{E}}{d\tilde{z}^2} + \epsilon_r \mathcal{E}^4 - S^2 = 0, \quad (3a)$$

$$\frac{dS}{d\tilde{z}} + \sigma_r \mathcal{E}^2 = 0, \quad (3b)$$

with boundary conditions

$$\left[\left(\mathcal{E} + \frac{S}{\mathcal{E}} \right)^2 + \left(\frac{d\mathcal{E}}{d\tilde{z}} \right)^2 \right]_{\tilde{z}=0} = 4, \quad (4a)$$

$$[S - \mathcal{E}^2]_{\tilde{z}=\tilde{d}} = 0, \quad (4b)$$

$$\left[\frac{d\mathcal{E}}{d\tilde{z}} \right]_{\tilde{z}=\tilde{d}} = 0. \quad (4c)$$

being $\epsilon_r = \epsilon/\epsilon_0$, the relative permittivity, and $\sigma_r = \sigma/(\epsilon_0 \omega)$, the relative conductivity. From Eq. (2) it is clear that S and \mathcal{E} are equivalents only when ϕ is a linear function on z . This point is not, in general, emphasized in the literature. Thereby, it is mandatory to ask: is the equivalence of both magnitudes generalized to cases where it could be not longer true?. An example: in Ref. [4], the energy flux of a TEM₀₀ Gaussian beam propagating in free-space is calculated from the squared-field amplitude modulus instead of the time-averaged Poynting vector which could lead to non-physical results. For details see Appendix A.

Equation (3b) represents the time-averaged Poynting Theorem being σ_r the responsible for the energy loss in the medium. Here we used it *explicitly* to analyze and solve wave propagation problems in bounded media. On the other hand, note that, Eqs. (4) are independent of the medium properties. Also, the second interface produces different values of \mathcal{E}^2 and S at the first interface through the spatial dependence of \mathcal{E} , as can be seen in Eq. (4a). However at the second interface \mathcal{E}^2 and S are always equals with the advertisement that this should not lead to false view that they are equivalents.

Finally note that, the energy conservation is guaranteed thorough the expression:

$$|r|^2 + |t|^2 = 1 - [S(0) - S(\tilde{d})]. \quad (5)$$

showing that the reflectance and transmittance values are limited by the boundary values of S and enhancing their importance in wave propagation problems in bounded media.

III. WAVE PROPAGATION ANALYSIS

A. Linear dielectric

The linear dielectric is the simplest nonabsorbent medium. It is clear from Eq. (3b) that the dimensionless

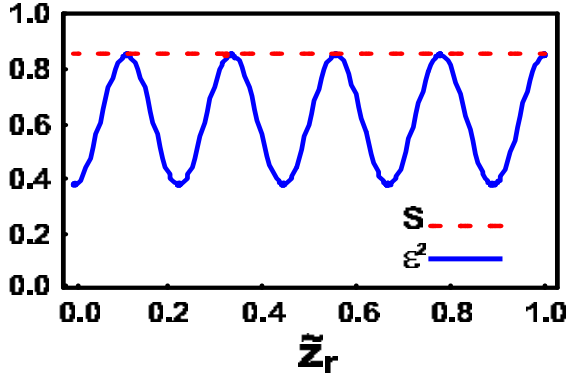


FIG. 2: (Color online) Spatial evolution of the dimensionless intensity S and squared-field amplitude modulus \mathcal{E}^2 for a linear dielectric. Clearly, S is a constant and \mathcal{E}^2 is an oscillatory function. The parameter values are $\sqrt{\epsilon_r} = 1.5$, $k_0 d = 3\pi$.

intensity S is a constant fixed by the boundary conditions when $\sigma_r = 0$. In this case, the analytical solutions for S and \mathcal{E}^2 are

$$S = \frac{1}{1 + F \sin^2(\delta/2)}, \quad (6a)$$

$$\mathcal{E}^2(\tilde{z}_r) = \frac{1 - (4F/(\epsilon_r - 1)) \sin^2[(1 - \tilde{z}_r)\delta/2]}{1 + F \sin^2(\delta/2)}, \quad (6b)$$

where $F = (\epsilon_r - 1)^2/(4\epsilon_r)$ is known as *finesse*, $\delta = 2\tilde{d}\sqrt{\epsilon_r}$ and $\tilde{z}_r = \tilde{z}/\tilde{d}$.

Equation (6a) is the transmittance result for the linear dielectric with Fabry-Perot geometry at normal incidence, i. e. the well-known Airy-formula [5]. The solutions (6) explicitly show that the intensity is nonequivalent to the squared-field amplitude modulus. Figure 2 points out the nonequivalence. The intensity is a

constant within the medium while the squared-field amplitude is an oscillatory function. Note that \mathcal{E} and S are only equals at $\tilde{z}_r = 1 - 2m\pi/\delta$ with $m \in \mathbb{N}$. Observe that when $\tilde{d} = m'\pi/\sqrt{\epsilon_r}$ ($m' \in \mathbb{N}$), $\delta = 2m'\pi$, then $\mathcal{E}(0) = S = 1$ attaining their maximum values ($T = 1$ and $R = 0$). In this case the medium behaves as a *delay sheet* transmitting all the incident intensity. When $\delta = (2m' + 1)\pi$ the field amplitude modulus and the temporal-averaged Poynting vector modulus attain their minimum values given by $\mathcal{E}(0) = [1 - 4F/(\epsilon_r - 1)]/(1 + F)$ and $S = 1/(1 + F)$. Note that, when ϵ_r increases, F also increases and the minimum of S diminishes.

On the other hand, when are both magnitudes really equivalents? When the squared-field amplitude modulus is a constant. In this case Eqs. (3) relate S and \mathcal{E} by

$$S = \sqrt{\epsilon_r} \mathcal{E}. \quad (7)$$

This case corresponds to the *single* plane wave propagating in an dielectric medium [2].

B. Linear absorber

The linear absorber or Ohmic conductor medium is characterized by $\sigma_r \neq 0$. Reference [1], for example, gives a rigorous analysis on the wave propagation at Fabry-Perot geometry within the counter-propagating wave approach. In this frame, additional steps are necessary since the time-averaged Poynting vector modulus is not derived from the amplitude modulus directly but from the Poynting vector definition. In turn, because the S-Formalism uses the radiation intensity as a field variable, its values at each point within the medium can be directly known and compared with the squared-field amplitude modulus once the evolution equations are solved. The solutions $S(z)$ and $\mathcal{E}^2(z)$ for the Ohmic conductor are derived from S-formalism evolution equations giving (For resolution details see Appendix B)

$$S(\tilde{z}_r) = 2 \frac{\alpha_+^2 \cosh[\alpha_- \tilde{d}(\tilde{z}_r - 1)] - \alpha_+ (\xi + 1) \sinh[\alpha_- \tilde{d}(\tilde{z}_r - 1)] + \alpha_-^2 \cos[\alpha_+ \tilde{d}(\tilde{z}_r - 1)] - \alpha_- (\xi - 1) \sin[\alpha_+ \tilde{d}(\tilde{z}_r - 1)]}{[\alpha_+^2 + (\xi + 1)^2] \cosh(\alpha_- \tilde{d}) + 2\alpha_+ (\xi + 1) \sinh(\alpha_- \tilde{d}) + [\alpha_-^2 - (\xi - 1)^2] \cos(\alpha_+ \tilde{d}) + 2\alpha_- (\xi - 1) \sin(\alpha_+ \tilde{d})}, \quad (8a)$$

and

$$\mathcal{E}^2(\tilde{z}_r) = 4 \frac{(1 + \xi) \cosh[\alpha_- \tilde{d}(\tilde{z}_r - 1)] - \alpha_+ \sinh[\alpha_- \tilde{d}(\tilde{z}_r - 1)] + (\xi - 1) \cos[\alpha_+ \tilde{d}(\tilde{z}_r - 1)] + \alpha_- \sin[\alpha_+ \tilde{d}(\tilde{z}_r - 1)]}{[\alpha_+^2 + (\xi + 1)^2] \cosh(\alpha_- \tilde{d}) + 2\alpha_+ (\xi + 1) \sinh(\alpha_- \tilde{d}) + [\alpha_-^2 - (\xi - 1)^2] \cos(\alpha_+ \tilde{d}) + 2\alpha_- (\xi - 1) \sin(\alpha_+ \tilde{d})}, \quad (8b)$$

where $\xi = |n_c|$ and $\alpha_{\pm} = 2_{Im}^{Re}\{n_c\}$ being n_c the complex refraction index given by $n_c = \sqrt{\epsilon_r + i\sigma_r}$. It verifies that Eq. (8) reduces to Eq. (6) for $\sigma_r \rightarrow 0$.

The solutions (8) are depicted in Fig. 3 for different relative conductivity values showing that the squared-field amplitude modulus could present a markedly oscillatory behaviour contrary to the intensity. Figure 3(a) shows the spatial evolution of both magnitudes for relatively small values of σ_r . Both decrease when the relative spa-

tial coordinate increases due to the medium absorption. The field attenuation is slight for small conductivity values which implies an intense contribution to the total field of the wave returning from the second interface producing a strong wave superposition. On the other hand, Fig. 3(b) was depicted for intermediary σ_r value. The field attenuation is sufficiently strong and the field amplitude modulus acquires a quasi-negligible value at inter-

face $\tilde{z}_r = 1$. However, this still produces a wave superposition so that \mathcal{E}^2 shows a slightly oscillatory decreasing behaviour. Thereby, the intensity and the squared-field amplitude modulus are yet nonequivalents. Finally, Fig. 3(c) was depicted for a relatively high value of σ_r . In this case, the field amplitude modulus is quite attenuated before to reach the interface $\tilde{z}_r = 1$. Then, the medium behaves as unbounded and both, the intensity and the squared-field amplitude, become completely equivalents verifying [6]

$$S(\tilde{z}_r) = \frac{\alpha_+}{2} \mathcal{E}^2(\tilde{z}_r). \quad (9)$$

In summary, Fig. 3 shows that the strength of wave superposition dynamic is directly related with the effect of the back interface which turns out in the nonequivalence of S and \mathcal{E}^2 .

IV. BEER'S LAW COMPARISON

The Beer's Law is commonly used to calculate the absorption coefficient by measuring the transmittance when the optical absorption within the medium is accounted. This law gives the intensity of the wave at interface $\tilde{z}_r = 1$ when the second interface effects are neglected [6]. Therefore, this Law is an approximate result since it consider only the first interface (only one boundary condition) to calculate the energy flux. The dimensionless intensity given by Beer's Law I_B attenuates exponentially as [6]

$$I_B(\tilde{z}_r) = S(0)e^{-\alpha_-\tilde{z}_r}, \quad (10)$$

where α_- characterize the absorptive medium properties (note that was used $S(0)$ instead of I_0 supposing that the intensity at $z_r = 0$ is know and it lead to diminish the differences with the exact result). Equation (10) was also depicted in Fig. 3 with the aim to compare the approximate Beer's Law intensity and the true intensity within the medium. It happens that $I_B(\tilde{z}_r)$ can departure from $S(\tilde{z}_r)$ for a wide range of usual parameters. Thereby, the exact transmittance $S(1)$ could differ from the approximated transmittance value $I_B(1)$ used often in experiments. It is clear that a difference appears when the second interface mediates in the wave dynamic, as Fig. 3(a) shows. When the effect of that interface is either quasi-negligible [Fig. 3(b)] or the medium can be considered as unbounded [Fig. 3(c)], both $I_B(\tilde{z}_r)$ and $S(\tilde{z}_r)$ do not present differences. Thereby, the validity of this approximation must be carefully tested for each particular problem since the difference $S(1) - I_B(1)$ depends on material parameters: ϵ_r , σ_r and \tilde{d} . In Fig. 4, the percentaged difference $I_B(1) - S(1)$ is shown. As it can see, there exist cases where the difference of both transmittances is approximately 10%. This major departure appears when the back interface effect is relevant i. e., when the wave superposition dynamic plays an

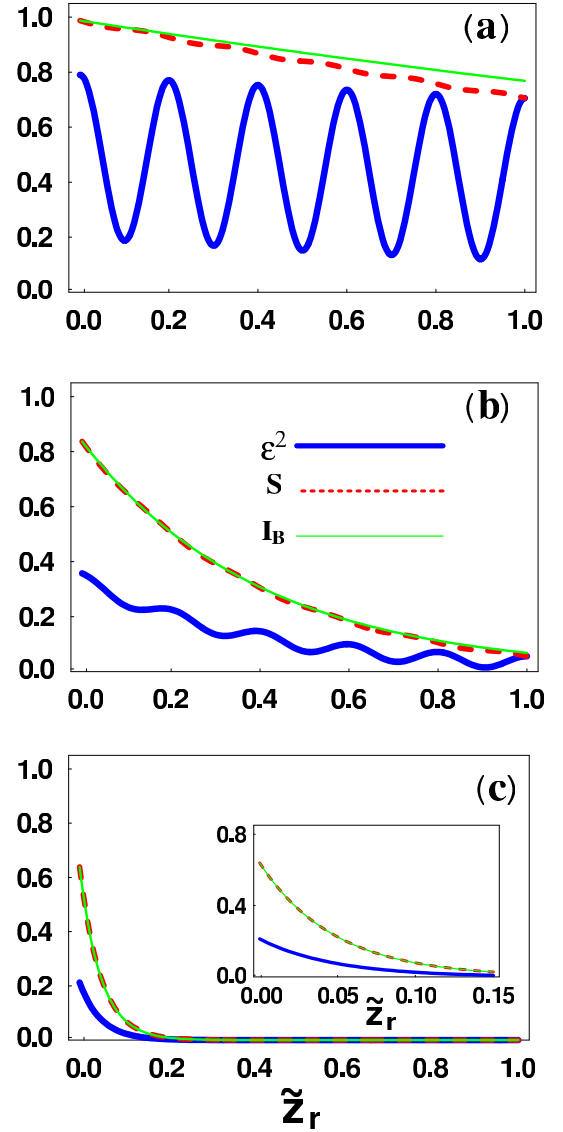


FIG. 3: (Color online) Spatial evolution of the dimensionless intensity S , squared-field amplitude modulus \mathcal{E}^2 , and Beer's Law intensity I_B for a linear absorber with different relative conductivity values: (a) $\sigma_r = 0.1$, (b) 1, (c) 10, with $\sqrt{\epsilon_r} = 2.5$, and $\tilde{d} = 2\pi$. Clearly, the non-equivalence between S and \mathcal{E}^2 is directly related to the effect of the second interface.

important role which happens only for certain particular values of (ϵ_r, σ_r) . Notice that, the maximum difference appears for high permittivity values and low, but nonzero, absorption.

V. REFLECTANCE OF POSITIVE AND NEGATIVE PERMITTIVITY MEDIA

Negative permittivity media have attracted the attention of scientist some years ago because was indicated a way to build them its [7] and because was open the possibility of have others media like the Left-handed Media

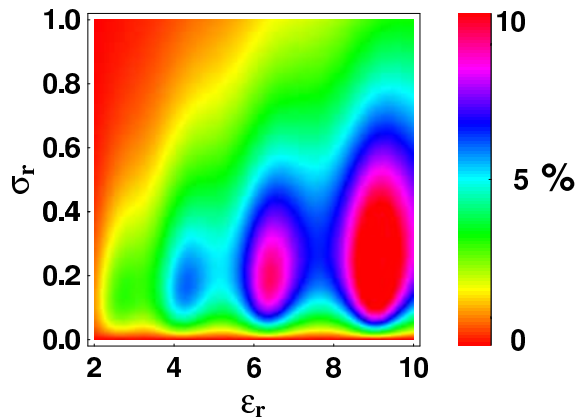


FIG. 4: (Color online) Percentaged difference $I_B(1) - S(1)$ against ϵ_r and σ_r for $\tilde{d} = 2\pi$.

[8] leading to a intense research in this area [9, 10, 11]. However, always the reflectance of negative permittivity media was analyzed in the context of the effective permittivity of a given microscopic configuration [7, 10]. Here we done a completely macroscopic analysis of the optical properties of positive and negative permittivity media without enter in the details of the microscopic configuration.

In Fig. 5.(a) the reflectance for both, positive and negative values of the relative permittivity is shown for several orders of magnitude of σ_r . By observing this figure, we found three regions well differentiated: (1) $\epsilon_r > 0$ and $\sigma_r < 1$; (2) $\epsilon_r < 0$ and $\sigma_r < 1$; (3) $\sigma_r > 1$. Region (1) is characterized by an oscillating low reflectance whose envelope grows as far as ϵ_r increases. This is a well-know behavior [1]: the reflectance of a low loss Fabry-Pérot. On the other hand, region (2) has a well particular dependence on ϵ_r and σ_r : the reflectance is close to unity. Finally, region (3) has a uniform reflectance as function of ϵ_r that grows monotonously as σ_r increases, such as in the limit $\sigma_r \gg 1$, $R \approx 1$ no matter the ϵ_r -value.

For a deeper understanding of the reflectance behavior we analyze the α_{\pm} dependence on ϵ_r and σ_r . Figures 5.(b) and 5.(c) depicts α_+ and α_- , respectively, as function of ϵ_r and σ_r . Also, in Table I the limiting values for $\sigma_r \ll (\gg) 1$ of α_{\pm}^2 and R are shown, to helping in the analysis. Note that, α_{\pm} represent the *effective* permittivity and conductivity in all the regions. Therefore, an analysis of these magnitudes becomes important for a better physical understanding on the wave dynamic propagation. In fact, these magnitudes determine the characteristics of the three region mentioned above, since their values changes dramatically in those. In region (1), $\alpha_+ \neq 0$ and $\alpha_- = 0$; in region (2) $\alpha_+ = 0$ and $\alpha_- \neq 0$; and in region (3) $\alpha_+ \approx \alpha_- \neq 0$. Then, the low and oscillatory reflection correspond to the region where α_+ predominates, i.e. the medium effectively behaves as a dielectric where the oscillations are produced by the wave superposition as result of the existence of the second interface summarizing in an Airy-type behavior, as Table I

TABLE I: Limiting values for α_{\pm}^2 and R for the three regions mentioned in the text.

	$\epsilon_r > 0; \sigma_r \ll 1$	$\epsilon_r < 0; \sigma_r \ll 1$	$\sigma_r \gg 1$
α_+^2	$4\epsilon_r$	0	$2\sigma_r$
α_-^2	0	$4 \epsilon_r $	$2\sigma_r$
R^a	$\frac{F \sin^2(\delta/2)}{1 + F \sin^2(\delta/2)}$	$\frac{F' \sinh^2(\delta/2)}{1 + F' \sinh^2(\delta/2)}$	$1 - 2\sqrt{2}/\sigma_r$
$^a F' = \frac{(\epsilon_r + 1)^2}{4 \epsilon_r }$			

shows. On the other hand, it is well-known that the high reflectance is commonly associated with high values of the conductivity, i.e for good conductors. However, high reflectance could occur even for low σ_r when the permittivity is negative. In this case, the response is dominated by α_- . The reflectance is given by a hyperbolic-Airy-type function as Table I show. Because $F' \sinh(\delta/2) \gg 1$ for almost all the ϵ_r -values in this region, then $R \approx 1$ and the medium posses mirror-like properties. For region (3), α_{\pm} strongly depend on σ_r -values. The medium response is completely dominated by σ_r with a reflectance that asymptotically reaches the unity with a moderately slow rate. Indeed, the asymptotic high reflection region is dictated by a unique parameter $\alpha \approx \alpha_+ \approx \alpha_-$. Summarizing, for region (1) is obtained a periodic function of ϵ_r for the reflectance, whereas for region (2) it contains sine hyperbolic functions that monotonously grow as ϵ_r decreases achieving rapidly the unity. Note that, although each reflectance was obtained by calculating the appropriate limit of Eq. (8), the reflectance in region (2) could be obtained from that of region (1) by changing $\epsilon_r \rightarrow -\epsilon_r$ what allows us to say that the propagation parameter α_+ “becomes” imaginary when the permittivity takes negative values doing that the medium behaves as a high absorbing one.

To end this section we stand out others interesting results: for $\epsilon_r = 1$, $R = 0$ because the medium is “matched” with the vacuum and all the light is transmitted; For $\epsilon_r = 0$ and $\sigma_r = 0$, $R = (1 + 4/\tilde{d})^{-1}$, showing that also in this “quasi-nihility” [12] some quantity of electromagnetic energy can propagate. And finally, note that for $\epsilon_r < 0$ and $\sigma_r \approx 1$ there exist a region where $R \approx 0.5$ showing that not all the negative permittivity media has a high reflectance, but those with $\sigma_r \ll 1$. Similar results were observer for low loss negative permeability media [9].

VI. CONCLUSIONS

The S-Formalism was used to study the wave propagation in bounded linear media. It utilizes the set (S, \mathcal{E}) as field variables instead of the conventional set (ϕ, \mathcal{E}) . Then, the electromagnetic energy flux can be directly known inside the medium. The approach stresses that, in general, the time-averaged Poynting vector modulus and

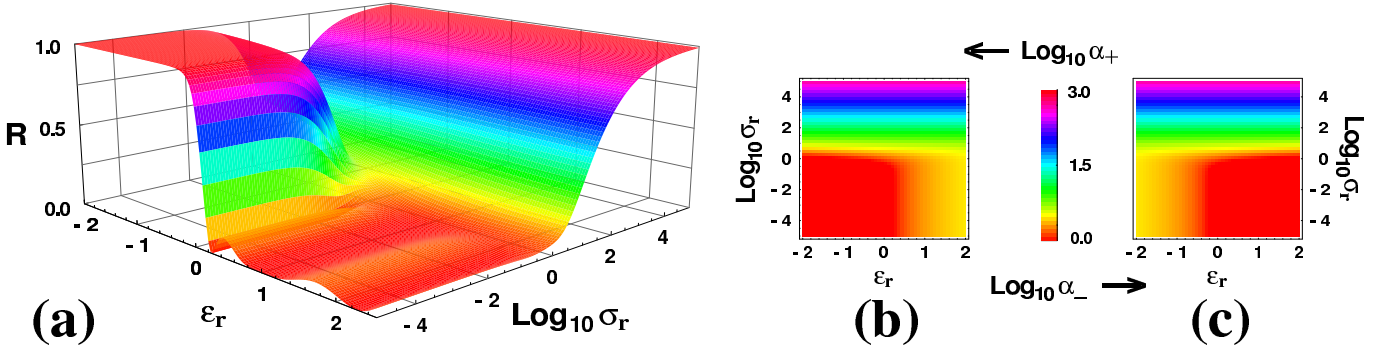


FIG. 5: (Color online) Reflectance (a), $\text{Log}_{10}\alpha_+$ (b), and $\text{Log}_{10}\alpha_-$ (c) against ϵ_r and $\text{Log}_{10}\sigma_r$. For reflectance $\tilde{d} = 2\pi$.

the squared-field amplitude modulus are non-equivalents. The analysis clearly shows that the non-equivalence of S and \mathcal{E}^2 takes place in bounded media being consequence of the back interface. The role of the latter is responsible for the superposition dynamic between the forward and backward waves which causes an oscillatory behaviour of the squared-field amplitude modulus contrary to the intensity. When the second interface can be neglected, the medium can be treated as unbounded with a single wave propagating such that S and \mathcal{E}^2 are equivalents. The analysis shows that the usual Beer's Law approximated intensity, employed to calculate the transmittance in usual experiments, could departure significantly from exact transmittance and this difference is also produced by the effect of the second interface. Thereby, the validity of this approximation should be rigourously tested for each particular problem. Moreover, positive and negative permittivity media were analyzed and found different behaviors accordingly to the permittivity and conductivity values. Was observed that, for low absorption, negative and positive permittivity media have a well differentiated reflectivity (being unity for the former and a low oscillating one for the later) whereas on the contrary case the reflectance does not depend on the permittivity values. For intermediate (moderate) absorption, the reflectance can take values around 0.5, showing that not all negative permittivity media have high reflectance.

Both methods, the conventional and the S-formalism, should be used complementarily what could help for a complete physical understanding on wave propagation in bounded linear media. The results for finite bandwidth waves can be easily obtained from the monochromatic ones by integrating all the contributions for the transmittance [13].

Acknowledgments

The authors thank Profs. N. Bolognini, H. R. Sandoval and G. M. Bilmes for helpful suggestions. A.L. thanks to CLAF-CNPq fellowship.

APPENDIX A: TRUE POWER OF A TEM₀₀ PARAXIAL GAUSSIAN BEAM

The free-space propagation of a TEM₀₀ Gaussian beam is a good example on two fundamental aspects: first, because the misconception about the equivalence of the squared-field amplitude modulus and the time-averaged Poynting vector exists in the literature and second, because by applying this misconception could lead to erroneous physical results.

The theoretical framework on Gaussian beams within the transverse field-paraxial approximation is well-known [4, 6]. The structure of a TEM₀₀ field amplitude, $E(x, y, z)$, propagating in free-space along z -axis with wave vector modulus k (towards $+z$) is [4, 6]

$$E = E_0 \frac{w_0}{w(z)} \exp \left[-\frac{x^2 + y^2}{w^2(z)} \right] \exp [ikz] \times \exp \left[-i \tan^{-1} \left(\frac{z}{z_0} \right) \right] \exp \left[ik \frac{x^2 + y^2}{2R(z)} \right] \quad (\text{A1})$$

here by simplicity we use dimensional coordinates. The Gaussian TEM₀₀ beam wavefront is perfectly flat at $z = 0$ acquiring, thus, curvature and begin spreading in accordance with

$$R(z) = \left[z + \frac{z_0^2}{z} \right], \quad w^2(z) = w_0^2 \left[1 + \left(\frac{z}{z_0} \right)^2 \right], \quad (\text{A2})$$

where $z_0 = kw_0^2/2$, and z is the distance propagated from the plane $z = 0$ where the wavefront is flat being w_0 the minimum spot size often called the waist radius. The parameters $w(z)$ and $R(z)$ are the spot size and the wavefront radius of curvature respectively after the wave has propagated a distance z [4, 6]. In Ref. 4, it has been emphasized that the energy per unit time crossing an infinite transverse plane ($z = cte$) should be a constant to meet the energy conservation for a losses medium. This calculus has been done considering equivalents the time-averaged Poynting vector and the squared-field amplitude modulus since

$$P_m = \frac{\epsilon_0 \omega}{2k} \int_{-\infty}^{\infty} \int_{-\infty}^{\infty} EE^* dx dy \quad (\text{A3a})$$

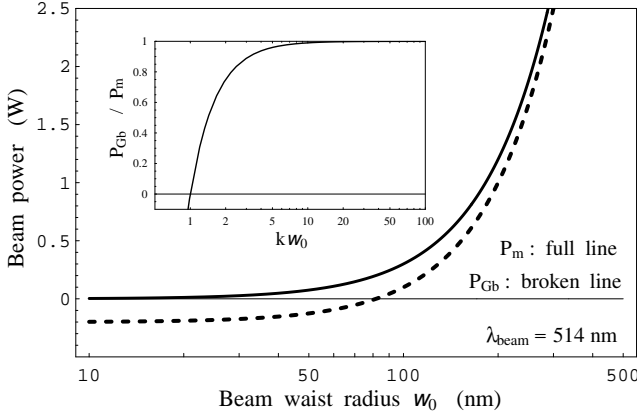


FIG. 6: Both, P_m and P_{Gb} Gaussian beam powers against waist radius for $E_0 = 1.2 \times 10^8$ V/m. The inset depicts the ratio among both powers as function of dimensionless parameter kw_0

was used giving the total power [4]:

$$P_m = \frac{\pi \varepsilon_0 \omega}{4k} w_0^2 E_0^2, \quad (\text{A3b})$$

which effectively is a constant. However, P_m does not represent the *truly* total power as it will be shown in the following. Necessarily, the power should be calculated from the time-averaged Poynting vector as

$$P_{Gb} = \int_{-\infty}^{\infty} \int_{-\infty}^{\infty} \langle S_z \rangle dx dy, \quad (\text{A4a})$$

where $\langle S_z \rangle$ is the z -component of the time-averaged Poynting vector given by Eq. (2). Calculating (A4a) it has

$$P_{Gb} = \frac{\pi \varepsilon_0 \omega}{4k} w_0^2 E_0^2 \left(1 - \frac{1}{k^2 w_0^2} \right), \quad (\text{A4b})$$

so that the power P_{Gb} is different of the power P_m accounted in the literature.

Figure 6 depicts P_{Gb} and P_m against the minimum spot size simulating an Argon laser beam. In most of the experimental cases, the beam wavelength is much lesser than that the beam waist radius satisfying $kw_0 \gg 1$. In these cases $P_{Gb} \approx P_m$, as the inset of Fig. 6 shows. It is clear that both power curves disjoin only from $kw_0 \lesssim 10$. This condition could be satisfied by ultra-focused beams [14]. In particular, note that, $kw_0 \leq 1$ leads to $P_{Gb} \leq 0$ (switch in the beam energy flux direction) which, of course, is a non-physical result. This unreal value of the total power P_{Gb} would be consequence of the fact that the transverse field-paraxial Gaussian beam approach are not longer valid. Thereby, the power curve P_{Gb} could be useful as measure parameter to evaluate when this theory can be used: when the P_{Gb} -value is far of the values equal and lesser than zero, i. e. when $P_{Gb} \approx P_m$. For the example placed in Fig. 6, this happens from $w_0 \approx 300$ nm. On the contrary, it is found that

always $P_m > 0$, which could lead to a misconception that this value represents the real beam power. The power curve P_m does not indicate when the theory fails. In summary, the departure of P_{Gb} from P_m could indicate the validity degree of the transverse field-paraxial Gaussian beam approach.

This simple example shows that the misconception about the equivalence of that magnitudes exists. In the literature, often, $|E|^2$ is used to calculate the intensity which could lead to erroneous physical results.

APPENDIX B: RESOLUTION OF EQS. (3)

Here is show the detailed resolution of Eqs. (3). Thus, the dielectric case is easily obtained making $\sigma_r = 0$.

Equations (3) can be written as:

$$2 \frac{d^2 u}{dz^2} u - \left(\frac{du}{dz} \right)^2 + 4 \epsilon_r u^2 = 4 S^2, \quad (\text{B1a})$$

$$\frac{dS}{dz} = -\sigma_r u, \quad (\text{B1b})$$

whit $u = \mathcal{E}^2$ and the boundary conditions reads

$$\left[\frac{du}{dz} \right]_{z=\tilde{d}} = 0, \quad (\text{B2a})$$

$$[S - u]_{z=\tilde{d}} = 0, \quad (\text{B2b})$$

$$\left[(u + S)^2 + \frac{1}{4} \frac{du}{dz} - 4u \right]_{z=\tilde{d}} = 0. \quad (\text{B2c})$$

By the homogeneity of the Eqs. (B1), we write down the following *ansatz*:

$$u = A \exp(a\tilde{z}), \quad (\text{B3a})$$

$$v = B \exp(a\tilde{z}). \quad (\text{B3b})$$

Replacing in Eq. (B1), it has

$$a^2 = \pm \alpha_{\mp}. \quad (\text{B4})$$

Then, the general solution can be written (*by the homogeneity of Eqs. (B1)*) as a linear combination of the four possible values of a :

$$u = A_1 \exp(\alpha_- \tilde{z}) + A_2 \exp(-\alpha_- \tilde{z}) + A_3 \exp(i\alpha_+ \tilde{z}) + A_4 \exp(-i\alpha_+ \tilde{z}) \quad (\text{B5a})$$

$$v = \frac{\alpha_+ \alpha_-}{2} \left[-\frac{A_1}{\alpha_-} \exp(\alpha_- \tilde{z}) + \frac{A_2}{\alpha_-} \exp(-\alpha_- \tilde{z}) + i \frac{A_3}{\alpha_+} \exp(i\alpha_+ \tilde{z}) - i \frac{A_4}{\alpha_+} \exp(-i\alpha_+ \tilde{z}) \right] \quad (\text{B5b})$$

The boundary conditions fix three of the four constants appearing in the solution, the fourth is fixed by auto-consistency. Replacing Eq. (B5a) in Eq. (B1a), it results

$$A_1 A_2 = A_3 A_4. \quad (\text{B6})$$

Applying the boundary conditions at $\tilde{z} = \tilde{d}$ and defining $B = A_1/A_3$, $C = A_2/A_3$, results $BC = A_4/A_3$, has

$$B = \left[\frac{2i\xi - (\alpha_- + i\alpha_+)}{2i\xi + (\alpha_- + i\alpha_+)} \right] \exp \left[(-\alpha_- + i\alpha_+) \tilde{d} \right], \quad (\text{B7a})$$

$$C = \left[\frac{2i\xi - (\alpha_- - i\alpha_+)}{2i\xi + (\alpha_- - i\alpha_+)} \right] \exp \left[(\alpha_- + i\alpha_+) \tilde{d} \right], \quad (\text{B7b})$$

and with the boundary condition at $\tilde{z} = 0$

$$A_3 = 4[B(1 + \xi - \alpha_+) + C(1 + \xi + \alpha_+) + BC(1 - \xi - i\alpha_-) + (1 - \xi + i\alpha_-)]^{-1}. \quad (\text{B8})$$

By replacing this values in Eq. (B5a), it gives

$$u = 4 \frac{(1 + \xi - \alpha_+) \exp[\alpha_- (\tilde{z}_r - 1)] + (1 + \xi + \alpha_+) \exp[-\alpha_- (\tilde{z}_r - 1)] + (\xi - 1 + i\alpha_-) \exp[-i\alpha_+ (\tilde{z}_r - 1)] + (\xi - 1 - i\alpha_-) \exp[i\alpha_+ (\tilde{z}_r - 1)]}{(1 + \xi - \alpha_+)^2 \exp[-\alpha_- \tilde{d}] + (1 + \xi + \alpha_+)^2 \exp[\alpha_- \tilde{d}] - (\xi - 1 + i\alpha_-)^2 \exp[i\alpha_+ \tilde{d}] - (\xi - 1 - i\alpha_-)^2 \exp[-i\alpha_+ \tilde{d}]}, \quad (\text{B9a})$$

and

$$v = 2 \frac{(1 + \xi + \alpha_+) \alpha_+ \exp[-\alpha_- (\tilde{z}_r - 1)] - (1 + \xi - \alpha_+) \alpha_+ \exp[\alpha_- (\tilde{z}_r - 1)] + i(\xi - 1 - i\alpha_-) \alpha_- \exp[i\alpha_+ (\tilde{z}_r - 1)] - i(\xi - 1 + i\alpha_-) \alpha_- \exp[-i\alpha_+ (\tilde{z}_r - 1)]}{(1 + \xi - \alpha_+)^2 \exp[-\alpha_- \tilde{d}] + (1 + \xi + \alpha_+)^2 \exp[\alpha_- \tilde{d}] - (\xi - 1 + i\alpha_-)^2 \exp[i\alpha_+ \tilde{d}] - (\xi - 1 - i\alpha_-)^2 \exp[-i\alpha_+ \tilde{d}]}. \quad (\text{B9b})$$

From this equations, Eqs. (8) can be obtained rearranging the exponential terms.

-
- | | |
|---|---|
| <p>[1] J.A. Stratton, <i>Electromagnetic Theory</i>, (McGraw-Hill, New York, 1941), p. 511–516.</p> <p>[2] J. D. Jackson, <i>Classical Electrodynamics</i>, 3rd. ed., (Jhon Wiley & Sons Inc. New York, 1999), p. 295–298.</p> <p>[3] A. Lencina and P. Vaveliuk, <i>Phys. Rev. E</i> 71, 056614(2005).</p> <p>[4] J. T. Verdeyen, <i>Laser Electronics</i>, (Prentice-Hall Inc., New Jersey, 1981) p. 61.</p> <p>[5] M. Born and E. Wolf, <i>Principles of Optics</i>, 6th ed., (Pergamon Press, New York, 1980) p. 60–62.</p> <p>[6] J. M. Cabrera, F. J. López and F. Agulló-López, <i>Óptica Electromagnética, Fundamentos</i>, (Addison-Wesley Iberoamericana, Wilmigton, 1993), p. 158–162.</p> <p>[7] J. B. Pendry, A. J. Holden, W. J. Stewart, and I. Youngs, <i>Phys. Rev. Lett.</i> 76, 4773(1996).</p> <p>[8] D. R. Smith, W. J. Padilla, D. C. Vier, S. C. Nemat-Nasser, and S. Schultz, <i>Phys. Rev. Lett.</i> 84, 4184 (2000);</p> | <p>R. A. Shelby, D. R. Smith, and S. Schultz, <i>Science</i> 292, 77 (2001).</p> <p>[9] S. O'Brien and J. B. Pendry, <i>J. Phys.: Cond. Matt.</i> 14, 4035(2002).</p> <p>[10] Ping Xu and Zhen-Ya Li, <i>J. Phys. D: Appl. Phys.</i> 37, 1718(2004).</p> <p>[11] Viktor, A. K. Sarychev, E. E. Narimanov and V. M. Shalaev, <i>J. Opt. A</i> 7, S32(2005); V. Yannopapas, and A. Moroz, <i>J. Phys.: Cond. Matt.</i> 17, 3717(2005); Yi-Fan Chen, P. Fischer, and F. W. Wise, <i>J. Opt. Soc. Am. B</i> 23, 45(2006).</p> <p>[12] A. Lakhtakia, <i>Int. J. Infrared Millim. Waves</i> 23, 813(2002).</p> <p>[13] A. Lencina and P. vaveliuk, unpublished.</p> <p>[14] R. Dorn, S. Quabis and G. Leuchs, <i>Phys. Rev. Lett.</i> 91, 233901(2003).</p> |
|---|---|